

# Dynamical complexity in the quantum to classical transition

Bibek Pokharel<sup>a</sup>, Peter Duggins<sup>(a)</sup>, Moses Misplon<sup>(a)</sup>, Walter Lynn<sup>(a)</sup>, Kevin Hallman<sup>(a)</sup>, Dustin Anderson<sup>(a)</sup>, Arie Kapulkin<sup>(b)</sup>, and Arjendu K. Pattanayak<sup>(a)</sup>

*(a) Department of Physics and Astronomy,*

*Carleton College, Northfield, Minnesota 55057*

*(b) 128 Rockwood Cr, Thornhill, Ont L4J 7W1 Canada*

(Dated: Thursday 3<sup>rd</sup> June, 2021)

## Abstract

We study the dynamical complexity of an open quantum driven double-well oscillator, mapping its dependence on effective Planck's constant  $\hbar_{eff} \equiv \beta$  and coupling to the environment,  $\Gamma$ . We study this using stochastic Schrodinger equations, semiclassical equations, and the classical limit equation. We show that (i) the dynamical complexity initially increases with effective Hilbert space size (as  $\beta$  decreases) such that the most quantum systems are the least dynamically complex. (ii) If the classical limit is chaotic, that is the most dynamically complex (iii) if the classical limit is regular, there is always a quantum system more dynamically complex than the classical system. There are several parameter regimes where the quantum system is chaotic even though the classical limit is not. While some of the quantum chaotic attractors are of the same family as the classical limiting attractors, we also find a quantum attractor with no classical counterpart. These phenomena occur in experimentally accessible regimes.

PACS numbers: 05.45.Mt,03.65.Sq

Investigations of how quantum behavior limits to (significantly different) classical dynamics inform quantum information, control, and technology. The limiting behavior is particularly intriguing for nonlinear systems: A generic classical nonlinear system (Hamiltonian or dissipative) can display dynamically complex behavior. The dynamical complexity includes in particular exponentially sensitive dependence on how precisely the initial condition is specified, visible in the distance  $d$  between initially close trajectories growing with time  $t$  as  $d(t) \approx d(t=0)e^{\lambda t}$ . Here  $\lambda$  is the Lyapunov exponent, one aspect of the Kolmogorov complexity of the dynamics. Closed quantum dynamics are entirely (quasi)-periodic, with no dynamically complex behavior (no positive  $\lambda$ ), yielding the paradox that chaotic classical Hamiltonians are a singular limit. Investigating this paradox and the singular limit greatly improved our understanding of semiclassical dynamics and also of the properties of quantum spectra and eigenfunctions as they relate to classical chaos [1].

However, nonlinear quantum systems are sensitive to environmental effects and their accurate description must include consideration of decoherence[2]. As such, further understanding of nonlinear effects in quantum dynamics emerged in studies of stochastic quantum trajectories, through conditioned measurement records or via the Quantum State Diffusion (QSD)[3] approach. Early work[4–6] showed that a classical phase-space chaotic attractor was recovered smoothly from quantum Poincaré sections for  $\langle \hat{Q} \rangle$  and  $\langle \hat{P} \rangle$  for a sufficiently small scaled Planck’s constant  $\hbar_{\text{eff}}(\equiv \beta \text{ below})$  and it disappeared slowly as  $\beta$  increases, Positive quantum  $\lambda$  have indeed been calculated [7], establishing that quantum complex dynamics exists. We are far from a complete understanding of this phenomenon however. Among many conjectures is the belief [8] that quantum effects suppress dynamical complexity in general and chaos and moreover, that quantum chaos exists only for systems which are classically chaotic. This dynamical complexity of quantum systems is of great interest to the field of quantum computing as well[9].

In this Letter, we investigate the dynamical complexity ( quantified below) of the open (dissipative) quantum Duffing system. Starting from high  $\beta$  (extreme quantum behavior) we find that the quantum system is always more dynamically complex than completely regular behavior (as for a classical periodic orbit). As  $\beta$  decreases so that the system becomes somewhat less quantal or more classical, the dynamical complexity of the system initially increases. This behavior transitions smoothly to the classical limit as  $\beta$  continues to decrease. However, since the classical behavior can be either be (I) chaotic attractors of high dynamical

complexity or (II) periodic orbits (dynamically simple behavior) we get two distinct results. For the case (I) the classical behavior is the most dynamically complex and for (II) there is a non-monotonic transition in that there is always a quantum system with complexity greater than the classical limiting behavior. The non-monotonic transitions include ‘anomalous’ examples of quantum chaos for systems with a periodic classical limit. Further, while some of these anomalous quantum chaotic attractors resemble the classically chaotic attractors at neighboring parameters, there are examples where the anomalous quantum chaotic attractors are unrelated to any classical dynamics. The last, to the best of our knowledge, is the first example of uniquely quantum chaotic attractors.

To understand this, we start by summarizing the classical behavior and its complexity; our particular system evolves as

$$\ddot{x} + 2\Gamma\dot{x} + \beta^2x^3 - x = \frac{g}{\beta}\cos(\Omega t), \quad (1)$$

representing a unit mass in a double-well potential, with dissipation  $\Gamma$  and a sinusoidal driving of amplitude  $g$  and frequency  $\Omega$ , and is termed the Duffing oscillator. Equation (1) is invariant under  $\beta \rightarrow \Lambda\beta; x \rightarrow \frac{x}{\Lambda}$  for any positive real  $\Lambda$ . We vary the dissipation parameter  $\Gamma$  and see the range of behaviors shown in the bifurcation diagram Fig. (1). This is constructed as follows: (a) fix  $\Gamma$ , (b) evolve an arbitrary initial condition over 200 periods of the driving, (c) discard the transients (10 drive periods) and record  $x$  ( $p$  can also be used with no change in the analysis) at  $t = 2n\pi$  for all  $n$  and (d) plot *all* the  $x(t = 2n\pi)$  results against  $\Gamma$ . These (and all results below) use a driving amplitude of  $g = 0.3$ . A chaotic orbit has  $x(t)$

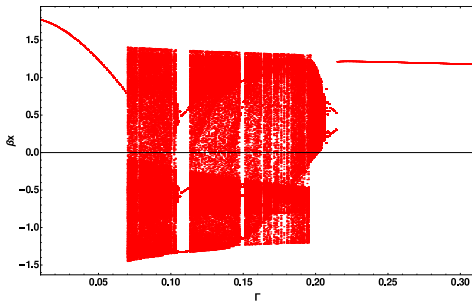


FIG. 1: Classical bifurcation diagram as a function of  $\Gamma$

wandering densely in phase space and looks like a solid line, while a regular (periodic) orbit yields just a few points. As  $\Gamma$  changes, chaotic attractors that persist with  $\Gamma$  look like a solid band, and periodic orbits that persist yield simple curves, as in Fig. (2). Also visible

are periodic-doubling cascades and transitions to (and from) chaos with  $\Gamma$ . The embedded regularity within generally chaotic dynamics results from higher-order symmetries emerging in the evolution equation. Such behavior, including the period doubling cascades, is generic in chaotic systems, though not always present[10]. All our calculations have non-zero  $\Gamma$  since  $\Gamma = 0$  is a singular Hamiltonian limit particularly for the quantum system.

This is quantified by the dynamical complexity  $K = \lambda + \Gamma$  plotted against  $\Gamma$  in Fig. (2); we also see  $K$  for various quantum systems, discussed below.  $K$  is the computational complexity quantifying the precision needed for the initial condition to get an accurate trajectory at some asymptotic time. For our system, phase-space lengths contract as  $\Gamma$  whence  $K$  correctly captures that given a globally attractive periodic orbit, zero information is needed about the initial condition to compute the entire future orbit.  $K$  is thus a measure of information needed about initial conditions for relative to this baseline for periodic orbits in dissipative systems. Finally, any system with  $K$  above the  $\Gamma$  diagonal has positive  $\lambda$  and is hence formally chaotic. We see that initially as  $\Gamma$  increases away from zero, the classical dynamics remain simple with  $K = 0$ . Around  $\Gamma_1 \approx 0.070$  there is an abrupt transition to complex behavior ( $K > 0$ ), which persists until  $\Gamma_2 \approx 0.210$ , except for the many small windows of regular behavior most prominently around  $\Gamma \approx 0.110$  for example. The figure thus shows the presence of one family of chaotic (complex) dynamical attractors, with the system switching between this and regular (simple) behavior. At low damping the global simple attractor is a periodic orbit moving in synchrony with the driving across both wells; the driving compensates for the dissipation.  $\Gamma_1$  marks when the dissipation is large enough such that the orbit does not always make it over the central potential barrier. This yields the potential for chaos: given two nearby orbits, one may cross the barrier while the other does not, leading to drastically different evolution. For  $\Gamma > \Gamma_2$  the damping is so high that the dynamics are restricted entirely to one of the wells, and does not yield complex behavior. We see that the  $K > 0$  ‘hill’ of complex dynamics arises from dynamics interacting with the central barrier of the potential; i.e., this ‘complexity hill’ marks a dynamical phase transition between simple behavior of differing symmetry. Thus, classically simple ( $K = 0$ ) dynamics corresponds to: (i) At low dissipation  $\Gamma < \Gamma_1$ , trivial double-well periodic orbits, (ii) at high dissipation  $\Gamma > \Gamma_2$ , trivial single-well periodic orbits, and (iii) at intermediate dissipation  $\Gamma_1 < \Gamma < \Gamma_2$ . high order periodic orbits in  $\Gamma$  windows of various sizes.

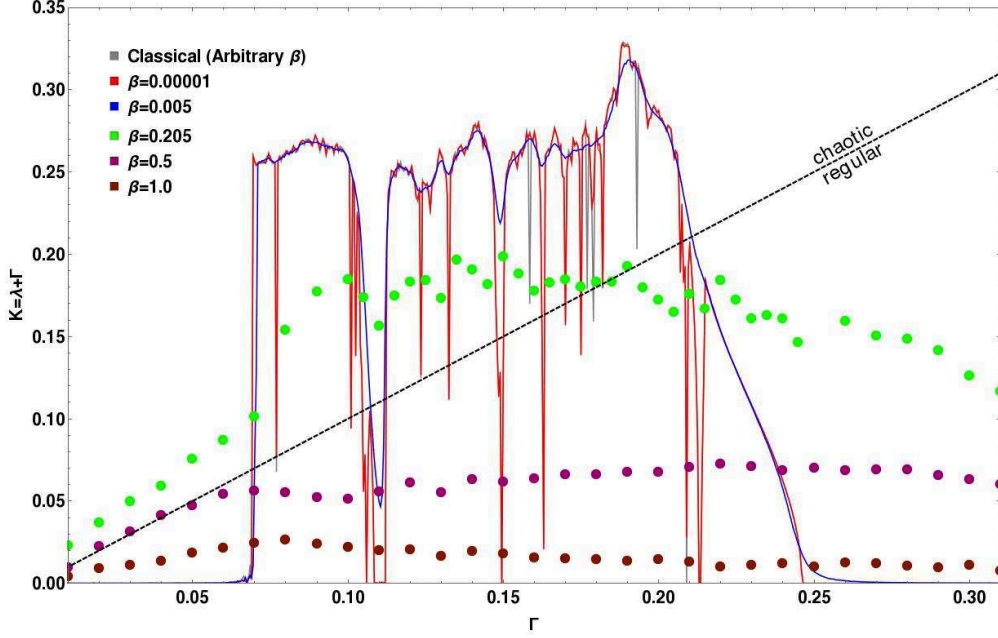


FIG. 2: Complexity  $K = \lambda_q + \Gamma$  vs  $\Gamma$  for various  $\beta$ .

The quantum dynamics are described by the Ito equation[3] for  $|\psi\rangle$  as

$$\begin{aligned}
 |d\psi\rangle = & -\frac{i}{\hbar}\hat{H}|\psi\rangle dt + \sum_j (\hat{L}_j - \langle \hat{L}_j \rangle) |\psi\rangle d\xi_j \\
 & + \sum_j \left( \langle \hat{L}_j^\dagger \rangle \hat{L}_j - \frac{1}{2} \hat{L}_j^\dagger \hat{L}_j - \frac{1}{2} \langle \hat{L}_j^\dagger \rangle \langle \hat{L}_j \rangle \right) |\psi\rangle dt
 \end{aligned} \quad (2)$$

where  $\hat{H}$  is the Hamiltonian and the  $\hat{L}_j$  are the Lindblad operators representing the action of a zero-temperature Markovian environment[3]. The  $d\xi_j$  are independent normalized complex differential random variables satisfying  $M(d\xi_j) = 0$ ;  $M(d\xi_j d\xi_{j'}) = 0$ ;  $M(d\xi_j d\xi_{j'}^*) = \delta_{jj'} dt$  where  $M$  represents the mean over realizations. This can be made dimensionless[5, 6, 11] with the Hamiltonian  $\hat{H}_\beta = \hat{H}_D + \hat{H}_R + \hat{H}_{ex}$  and a Lindblad operator  $\hat{L}$  for Eq. (2), where  $\hat{H}_D = \frac{1}{2}\hat{P}^2 + \frac{\beta^2}{4}\hat{Q}^4 - \frac{1}{2}\hat{Q}^2$ ,  $\hat{H}_R = \frac{\Gamma}{2}(\hat{Q}\hat{P} + \hat{P}\hat{Q})$ ,  $\hat{H}_{ex} = -\frac{g}{\beta}\hat{Q}\cos(\Omega t)$ ,  $\hat{L} = \sqrt{\Gamma}(\hat{Q} + i\hat{P})$ . Both the quantum nonlinearity and the dissipation scale with  $\Gamma$ , via  $\hat{L}$ .  $\beta$  is dimensionless and related to the original system's parameters of mass  $m$ , length  $l$ , and natural frequency  $\omega_0$  as  $\beta^2 = \frac{\hbar}{ml^2\omega_0}$  and serves as  $\hbar_{\text{eff}}$  determining the scale (and degree of 'quantumness') of the system[5, 6]. That is, increasing  $\beta$  amounts to a smaller system needing fewer quantum states to describe the dynamics, and  $\beta \rightarrow 0$  is thence the classical limit. Recently analysis[13] shows that experimentally accessible nano-electromechanical systems (NEMS) are well described by this model with parameters of recent experiments within range of the phenomena we

report.

To fully map the quantum-classical transition, we also consider the semiclassical dynamics ([6, 12] ) derived from the evolution equations for  $\langle \hat{Q} \rangle, \langle \hat{P} \rangle$ . These include their dependence on second moment terms  $\sigma_{QQ}, \sigma_{PP}, \sigma_{PQ}$  as well as the environmental term  $d\xi$ , where  $\sigma_{AB} = \langle (\hat{A}^\dagger - \langle \hat{A} \rangle^*)(\hat{B} - \langle \hat{B} \rangle) \rangle$ . The second moments are themselves time dependent and depend on higher order terms like  $\sigma_{QQQ}$  etc. An infinite hierarchy[14] of time dependent moments corresponds to the full quantum dynamics. Various approximations exist[15]; we truncate at the second order, leaving us

$$dx = pdt + 2\sqrt{\Gamma}((\mu - \frac{1}{2})d\xi_R - Rd\xi_I) \quad (3)$$

$$dp = (-\beta^2(x^3 + 3\mu x) + x - 2\Gamma p + \frac{g}{\beta}\cos(\omega t))dt + 2\sqrt{\Gamma}(Rd\xi_R - (\kappa - \frac{1}{2})d\xi_I) \quad (4)$$

$$\frac{d\mu}{dt} = 2R + 2\Gamma(\mu - \mu^2 - R^2 + \frac{1}{4}) \quad (5)$$

$$\frac{d\kappa}{dt} = 2R(-3\beta^2 x^2 + 1) + 2\Gamma(-\kappa - \kappa^2 - R^2 + \frac{1}{4}) \quad (6)$$

$$\frac{dR}{dt} = \mu(-3\beta^2 x^2 + 1) + \kappa - 2\Gamma R(\mu + \kappa), \quad (7)$$

where  $\langle \hat{Q} \rangle \equiv x, \langle \hat{P} \rangle \equiv p \equiv \dot{x}, R \equiv \frac{1}{2}(\sigma_{QP} + \sigma_{PQ}), \sigma_{QQ} \equiv \mu$  and  $\sigma_{PP} \equiv \kappa$ . Equations (4,5) contain the classical Eq. (1), along with quantum terms. The first of these depends on  $\mu$  and arises from  $\hat{H}$  being nonlinear. Other terms emerge via  $\hat{L}$  and depend on  $\sqrt{\Gamma}d\xi$  and  $\sigma(= \mu, \kappa, R)$ . As  $\beta \rightarrow 0$  the range of  $x, p$  increases as  $\frac{1}{\beta}$  while  $\sigma$  and  $d\xi$  terms remain unchanged in scale (of order unity). Thus, as  $\beta$  decreases, the product terms like  $\simeq \sigma d\xi$  quickly become relatively negligible, followed by the separate  $\sigma, d\xi$  terms, and these equations reduce to the classical Eq. (1) for a point particle, identified with  $(x, p)$ , the quantum centroid.

This scaling of various moments is consistent with and justifies the semiclassical truncation. The semiclassics can be variously validated, most simply by comparing with the full quantum evolution. For a given parameter set, as  $\beta$  decreases from some value (say  $\simeq 0.1$  for this system), once the semiclassics agree with the full quantum dynamics at some  $\beta_{sc}$  they can only *improve* in accuracy for  $\beta < \beta_{sc}$ . This depends on system parameters in interesting ways, but is empirically found to be greater than  $\beta \simeq 0.01$ . The full quantum calculations scale in computational difficulty as roughly  $\exp(\beta^{-3})$ . We have deployed two implementations (the QSD library[3] using a moving basis technique efficient at higher  $\Gamma$  and low  $\beta$ ,

and a fixed basis XMDS2[16] method which performs better at lower  $\Gamma$  and higher  $\beta$ ), along with semiclassics at even lower  $\beta$ , to cover the full range reported.

To compute the quantum  $\lambda$ , a fiducial  $\psi_{fid}$  and perturbed  $\psi_{per}$  with  $\psi_{per}$  created by a random small unitary kick applied to  $\psi_{fid}$ , are evolved with identical noise realizations. Then  $\lambda = \lim_{t \rightarrow \infty} \lim_{\Delta x(0), \Delta p(0) \rightarrow 0} \frac{1}{t} \log_2 \left( \sqrt{\frac{(\Delta x(t))^2 + (\Delta p(t))^2}{(\Delta x(0))^2 + (\Delta p(0))^2}} \right)$  where  $\Delta x(t) = \langle \hat{Q} \rangle_{\psi_{fid}} - \langle \hat{Q} \rangle_{\psi_{per}}$  and similarly  $\Delta p(t)$ . As is canonical[17], the limit of infinite time and zero initial distance is replaced by the perturbed trajectory being periodically reset to remain within the linear deviation regime, and the logarithmic rate of change of distance before every reset is averaged. To ensure convergence, the  $\lambda$  are computed over 3000 periods of the driving, and averaged over multiple noise realizations.

Figure (2) summarizes our central results, comparing  $K$  for (i) the classical system, (ii)  $\beta_1 = 0.00001$ , the extreme semi-classical limit, (iii)  $\beta_2 = 0.02$ , (iv)  $\beta_3 = 0.205$ , (v)  $\beta_4 = 0.5$ , and finally (vi) an extreme quantum version at  $\beta_5 = 1.0$ . The quantum  $K$  versus  $\Gamma$  results can be summarized as follows: (a) They broadly resemble the classical and differ increasingly with increasing  $\beta$ . (b) For any  $\Gamma$ ,  $K$  starts low at  $\beta = 1.0$  and increases with decreasing  $\beta$  at least through  $\beta \approx 0.2$ . (c) If the classical limit is chaotic,  $K$  is the greatest for the classical system, (e) For all other cases,  $K$  is non-monotonic with  $\beta$  such that there is always a quantum system more dynamically complex than the classical limit.

The initial increase in  $K$  as  $\beta$  decreases from 1.0 results from the increase in size of the effective Hilbert space of the dynamics. That is, at  $\beta \approx 1.0$  the dynamics are described by two or so quantum states, hence with low dynamical complexity and low  $K$  (though not as simple as classical periodic orbits); the number of states increases with  $\beta^{-1}$ , as numerically verified by us. This holds true even at  $\Gamma$  values corresponding to the ‘complexity hill’, which flattens ( $K$  decreases) as  $\beta$  increases since the central barrier matters less due to tunneling effects. As with the classical dynamics, the  $\Gamma$  dependence at a given  $\beta$  is quite complicated. Generically (this is most visible at intermediate  $\beta = 0.205$ ),  $K$  increases with  $\Gamma$  initially due to the  $\Gamma$  dependence of the nonlinearity in Eq. (2). We then have the jump in  $K$  as with the classical system for the ‘complexity hill’, followed by a slow decrease as  $\Gamma$  increases; this last arises from tunneling effects delaying the dissipative transition to single-well dynamics for quantum systems. In looking at the transition of the quantum behavior to the classical limit, for small enough  $\beta$  the quantum results trace the classical curve, including the return to  $K = 0$  at the low and high  $\Gamma$  values, *and* in the narrow windows in the intermediate

$\Gamma$  regime. The number of  $\Gamma$  windows where the classical and quantum results disagree decrease as  $\beta$  decreases; the  $\beta = 0.00001$  results illustrate this, but we emphasize that we have recovered the classical limit for *all*  $\Gamma$  values. Considering in particular chaos ( $\lambda$ ) rather than  $K$ , therefore, the quantum-to-classical transition can be anomalous in being regular-to-chaotic instead of the usual chaotic-to-regular; this happens in all three regimes where classically regular behavior exists.

The anomalous behavior in the intermediate dissipation regime (e.g. for  $\Gamma = 0.110$ ) is understood semiclassically by comparing Eqs. (5-9) with the classical Eq. (1) when the spread variables ( $\mu, \kappa, R$ ) are relatively small. The dynamics of these spread variables when coupled to the centroid motion can destroy the delicate classical periodic orbits, with the effects increasing with  $\beta$ . The narrowest windows – where the smallest change to the dynamical equations sends the system back into chaos – are naturally the most difficult to reproduce quantum mechanically or semiclassically; the perturbative effect of the quantum variables destroys the classical regularity in these windows. The quantum (semiclassical) attractor in these situations has essentially the same  $K$  as the classical chaotic attractor family and is visually essentially identical. This is clear in the Poincare sections shown in Fig. (3), constructed by periodically recording  $(x(t), p(t))$  once every driving period, i.e. at  $t = 2n\pi$  for all  $n$ . We see regular classical behavior destroyed by the quantum mechanics which ‘recovers’ the classically chaotic attractor (to be compared with, for example, the classical attractor in Refs. [5, 6, 11]). Similiar anomalous chaos also obtains for  $\Gamma \approx 0.209$ . Physically, the classical trajectory is regular since it is dissipatively constrained to one well. As  $\beta$  increases quantum tunneling yields a quantum chaotic attractor resembling the classical attractor, (see Fig. (4)) with quantum  $K$  values essentially the same as for the classical attractors. We note that these results also confirm that even at  $\Gamma = 0.3$ , intermediate  $\beta$  systems have greater  $K$  values than the classical system even though they are not chaotic[11].

Finally, at low damping  $\Gamma < 0.07$  there is also quantum chaos (see the  $\beta = 0.205$  curve) that does not exist classically. As evidence that this is not ‘recovered’ classical chaos, but is uniquely quantal we note: Both  $K, \lambda$  differ substantially from that for the other chaotic attractors (classical and quantum), as does the Poincare section (Fig. (5)). Also, unlike the other cases, the phase-space contracts for the chaotic attractor ( $\lambda > 0$ ) compared to when  $\lambda < 0$ . At  $\Gamma = 0.05$  this transition happens as  $\beta$  increases beyond  $\approx 0.12$ . At this

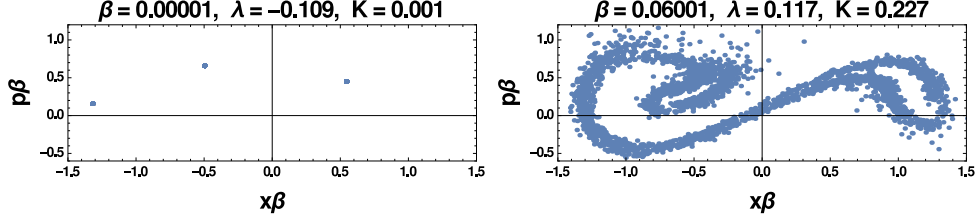


FIG. 3: Poincare maps for  $\Gamma = 0.11$

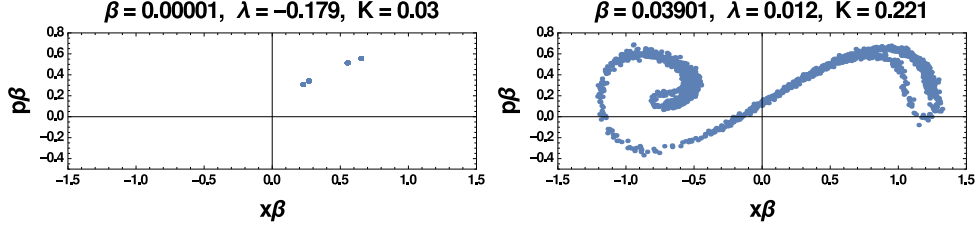


FIG. 4: Poincare maps for  $\Gamma = 0.209$

$\beta$  semiclassics are clearly not valid, but the structure of Eqs. (5-7) for  $\mu, \kappa, R$  is instructive. Starting with  $\beta$  near 0 and briefly ignoring the  $\Gamma$  terms, we have three linear equations with a constant of motion ( $R^2 - \mu\kappa$ ). At these  $\Gamma$  values, the  $\Gamma$  terms are first order corrections, and effectively add more linear terms which cannot engender chaos. However, as  $\beta$  increases, the  $\beta^2 x^2$  term creates a discernible nonlinear coupling between Eqs. (3-4) and Eqs. (5-7) and breaks the integrability. This is essentially the same as for the previous anomalous chaos, but here it happens at intermediate  $\beta$ , and does not restore a classical-like chaotic attractor. Accurate semiclassics in this  $\beta$  regime include more terms and equations of higher  $\beta$  order. However, those higher terms are not necessary for chaos since both the semiclassical system Eqs. (3-7) and the full quantum system Eq. (2) are chaotic in this  $\beta$  regime, such that the semiclassics are qualitatively valid. This is uniquely quantum trajectory chaos, without a corresponding classical attractor. The ingredients for this anomaly are sufficient

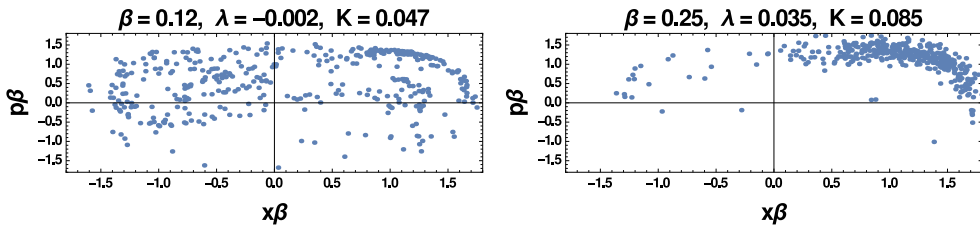


FIG. 5: Poincare maps for  $\Gamma = 0.05$

quantum nonlinearity (size of Lindblad terms), and intermediate  $\beta$  (so the Hilbert space is large enough to not be too simple but  $\beta$  is not so small as to track classical regularity) and this should be a generic phenomenon. Interesting avenues for further investigation include the dependence of the break point ( $\beta_{sc}$ ) on  $\Gamma$  and the degree of classical or quantum chaos. We have already seen examples where the semiclassics works better for a system with greater classical chaos compared to a system that is classically regular, contrary to standard intuition.

Our results show that the dynamical complexity across the quantum-to-classical transition for open nonlinear quantum systems is substantially richer than the current intuition that quantum effects cause classically chaotic and dynamically complex behavior to transition to quantum regularity and simple behavior. The details depend strongly on system particulars. In general the quantum evolution is dynamically complex, and this means that if the classical limit is regular, the deeper quantum regime may display chaos that does not exist in the classical limit. In particular, as in the intermediate dissipation regime where the classical system has regular behavior corresponding to higher-order dynamical symmetry, the classical regular behavior can be difficult to recover – we have to go to larger and larger length scales (smaller  $\beta$ ) to recover correspondence. That is, ironically contrary to the standard wisdom[1], the correspondence limit can be most difficult for certain classically regular systems. How much of this behavior depends on the specific choice of Lindblad operator (that is, the exact form of the relevant stochastic Schrodinger equation) is an intriguing question currently being investigated[18]. It is already clear that the broader parameter regimes in question for this and other explorations are within reach of current experiments[13].

A.K.P. is grateful for funds from the HHMI through Carleton and the hospitality of J.M. Röst at MPIPKS in Dresden, G. Mantica at CNCS at the University of Insubria in Como, as well as of KITP at Santa Barbara, and helpful conversations with A. Carvalho.

---

[1] L.E. Reichl, *The Transition to Chaos in Conservative Systems: Quantum Manifestations*, 2nd edition (Springer, New York 2004); F. Haake, *Quantum Signatures of Chaos*, (Springer, Berlin, 2010).

[2] E. Ott, T.M. Antonsen, Jr, and J.D. Hanson, Phys. Rev. Lett. **53**, 2187 (1984); T. Dittrich,

- and R. Graham, *Europhys. Lett.* **4** 263 (1987); B.G. Klappauf, W.H. Oskay, D.A. Steck, and M.G. Raizen, *Phys. Rev. Lett.* **81**, 1203 (1998); **82**, 241 (E) (1998); H. Ammann, R. Gray, I. Shvarchuck, and N. Christensen, *Phys. Rev. Lett.* **80**, 4111 (1998); S. Habib, K. Shizume, and W.H. Zurek, *Phys. Rev. Lett.* **80**, 4361 (1998); A.K. Pattanayak, B. Sundaram, and B.D. Greenbaum, *Phys. Rev. Lett.* **90**, 014103 (2003); J.B. Gong and P. Brumer, *Phys. Rev. A* **68**, 062103 (2003).
- [3] I.C. Percival, *Quantum State Diffusion* (Cambridge University Press, Cambridge, England, 1998).
- [4] T.P. Spiller and J.F. Ralph, *Phys. Lett. A* **194**, 235(1994).
- [5] T.A. Brun, I.C. Percival, and R. Schack, *J. Phys. A* **29**, 2077 (1996).
- [6] Y. Ota and I. Ohba, *Phys. Rev. E* **71**, 015201(R) (2005).
- [7] T. Bhattacharya, S. Habib, and K. Jacobs, *Phys. Rev. Lett.* **85**, 4852 (2000); S. Habib, K. Jacobs and K. Shizume, *Phys. Rev. Lett.* **96**, 010403 (2006); S. Ghose, P. M. Alsing, I. H. Deutsch, T. Bhattacharya, S. Habib, and K. Jacobs, *Phys. Rev. A* **69**, 052116 (2004).
- [8] J. Finn, K. Jacobs, B. Sundaram, *Phys. Rev. Lett.* **102**, 119401 (2009); K. Kingsbury, C. Amey, A. Kapulkin, and A.K. Pattanayak *Phys. Rev. Lett.* **102**, 119402 (2009).
- [9] D.K.Burgarth,P.Facchi,V.Giovannetti,H.Nakazato,S.Pascazio, and K.Yuasa, *Nat. Commun*, **5**, 5173 (2014).
- [10] See for example the recent paper E. Sander and J.A. Yorke, *Chaos* **23**, 033113 (2013).
- [11] A. Kapulkin and A.K. Pattanayak, *Phys. Rev. Lett.* **101**, 074101 (2008).
- [12] J. Halliwell and A. Zoupas, *Phys. Rev. D* **52**, 7294 (1995).
- [13] Q. Li, A. Kapulkin, D. Anderson, S.M. Tan, and A.K.Pattanayak, *Phys. Scr.* T151 014055 (2012).
- [14] M. Andrews, *J. Phys. A* **14**, 1123 (1981).
- [15] A.K. Pattanayak and W. Schieve, *Phys. Rev. E* **50**, 3601 (1994).
- [16] G.R. Dennis, J.J. Hope, and M.T. Johnsson, *Comput. Phys. Commun.* **184**, 201 (2013).
- [17] A. Wolf, J.B. Swift, H.L. Swinney, and J.A. Vastano, *Physica D* **16**, 285 (1985).
- [18] J.K. Eastman,J.J. Hope,and A.R.R. Carvalho (unpublished)